Solar Energy 170 (2018) 212–216

Contents lists available at ScienceDirect

Solar Energy

journal homepage: www.elsevier.com/locate/solener

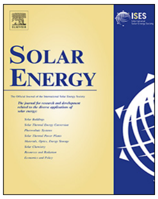

Improved charge transport ability of polymer solar cells by using NPB/MoO_3 as anode buffer layer

Ping Li[a,b,c], Bo Wu[a], You Chang Yang[a], Hai Shen Huang[a], Xiu De Yang[a,b,c], Guang Dong Zhou[b,c], Qun Liang Song[b,c,*]

[a] *School of Physics and Electronic Science, Zunyi Normal University, Zunyi 563006, PR China*
[b] *Institute for Clean Energy and Advanced Materials, Faculty of Materials and Energy, Southwest University, Chongqing 400715, PR China*
[c] *Chongqing Key Laboratory for Advanced Materials and Technologies of Clean Energy, Chongqing 400715, PR China*

ARTICLE INFO

Keywords:
Polymer solar cells
NPB
MoO_3
Hole extraction layer

ABSTRACT

Efficient polymer solar cells were fabricated with regioregular poly 3-hexylthiophene (P3HT):(6,6)-phenyl C61 butyric acid methyl ester (PCBM)) as active layer and molybdenum trioxide (MoO_3) and (N,N′-diphenyl)-N,N′-bis(1-naphthyl)-1,1′-biphenyl-4,4′-diamine (NPB) as buffer layers. The results of transient photocurrent and electrochemical impedance spectrometry of device indicate that the insertion of NPB layer between the active layer and MoO_3 layer is critical to the enhanced performance. It can effectively prevent charge recombination at the interface of MoO_3 hole extraction layer, reduce interfacial resistance due to the formation of Ohmic contact and enhance the exciton dissociation because of the newly formed NPB/PCBM dissociation interface. The optimized thickness of NPB layer is 5 nm, resulting in maximized power conversion efficiency (PCE) of 3.94% under AM1.5G 100 mW cm^{-2} illumination.

1. Introduction

Organic solar cells (OSC) with a great potential for large area, low cost, light weight, various function materials and highly processable flexibility, are regarded as one of the candidates of next generation renewable energy (Zhang et al., 2017; Lima et al., 2016). Up till now, even over 13% of power conversion efficiency (PCE) has been reported (Xu et al., 2018; Zhao et al., 2017), it still cannot meet the requirement for industrialization. Many methods have been developed to improve the PCE of OSCs, such as the synthesis of multifunctional organic materials, the design of different device structures, the introduction of interfacial layer between the electrode and the active layer, and the application of additives into active layer and so on (Jang et al., 2016; Lim et al., 2017; Jia et al., 2017). The using interfacial layer is very simple and effective to enhance the PCE of OSCs (Lim et al., 2017; Jia et al., 2017). Chen et al. reported that the insertion of cesium carbonate (Cs_2CO_3) as the cathode buffer improves the PCE of device from 2.3% to 3.1% (Chen et al., 2008). He et al. demonstrated that PCE of OSCs can be further enhanced to 9% by using an alcohol-/water-soluble conjugated polymer (PFN) as the cathode interfacial layer (He et al., 2012). In addition, metal oxides, such as ZnO and TiO_2, are widely used as the cathode interfacial layers to achieve high efficiency devices (Pali et al., 2017; Bandara et al., 2011).

Meanwhile, many metal oxides were developed as anode interfacial layer to be applied in OSC, such as molybdenum trioxide (MoO_3), vanadium oxide (V_2O_5), nickel oxide (NiO), p-type FeOx film (Xie et al., 2013; Jiang et al., 2015; Huang et al., 2018). Jiang et al. demonstrated p-type NiO can be prepared by a facile chemical precipitation method under room-temperature. Compared with conventional PEDOT:PSS-buffered devices, the NiO-buffered OSCs achieved improved or comparable device performances (Jiang et al., 2015). By introducing the strong electron acceptor (Cheng et al., 2018) or graphene (Cheng et al., 2017), the work function of NiO or the conductivity of NiO was continuously tuned/improved, enhancing the efficiency and stability of OSC ultimately.

The most widely commonly used anode interfacial layer is MoO_3, which possesses advantages of good hole conductivity and high work function (Elumalai et al., 2013; Greiner et al., 2012). Besides single layer MoO_3, double-layer or hybrid buffer layer based on MoO_3 were carried out to further enhance the performance and stability of OSCs (Cheng et al., 2011; Jin et al., 2013; Wang et al., 2015). Li et al. demonstrated that the very good device performance was achieved by using the Cs doped MoO_3 as hole anode interfacial layer, which was attributed to the work function of MoO_3 tuned by intercalating Cs to match the highest occupied molecular orbital (HOMO) of polymer donor. The film formation is also a simple room temperature solution

---

[*] Corresponding author at: Institute for Clean Energy and Advanced Materials, Faculty of Materials and Energy, Southwest University, Chongqing 400715, PR China.
E-mail address: qlsong@swu.edu.cn (Q.L. Song).

https://doi.org/10.1016/j.solener.2018.04.020
Received 7 March 2018; Received in revised form 9 April 2018; Accepted 11 April 2018
0038-092X/ © 2018 Elsevier Ltd. All rights reserved.

process (Li et al., 2014a,b). Cheng et al. reported that a thin layer of CuPc introduced between MoO_3 layer and Poly(3-hexylthiophene) (P3HT): (6,6)-phenyl C61 butyric acid methyl ester (PCBM)) active layer can enhance spectral coverage, and thus finally enhance the performance of device (Cheng et al., 2011). Jin et al. demonstrated that the PCE and lifetime of OSCs could be enhanced by using bathophenanthroline (Bphen) and MoO_3 as a compound anode buffer layer (Jin et al., 2013). In order to solve the aggregation of MoO_3 nanoparticles in solution, MoO_3 precursor solution was prepared by mixing with PEDOT:PSS to form compound hole transporting layer (HTL), achieving a high efficiency and long-term stability device (Wang et al., 2015). To further improve the conductivity of MoO_3 film, Ag-MoO_3 composite film was prepared by introducing the Ag nanoparticle into MoO_3 solution, boosting the PCE to 4.3% (Li et al., 2013).

NPB has been widely used as HTL in OSCs and organic light-emitting diodes (Gong et al., 2013; Mu et al., 2013). It is also reported that excitons at the organic interface in OSCs can be effectively dissociated by NPB interface (Huang et al., 2012; Chen et al., 2015). Considering the capability of NPB to dissociate excitons, it is very promising to achieve high efficiency device by the insertion of NPB between MoO_3 and photoactive layer in OSCs. Li et al. (2016) has recently applied NPB with MoO_3 to form a double-layer HTL, the PCE of OSCs were improved from 2.63% to 2.96%. However, the NPB was inserted between MoO_3 and electrode in that study, not direct contact with the active layer. Thus the ability of exciton dissociation of NPB could not be used. The double-layer of NPB/MoO_3 was also demonstrated as an effective interfacial layer in perovskite solar cells, with NPB contact directly with perovskite layer. The high open circuit voltage (V_{oc}) obtained by this configuration indicates the well match of the HOMO level of NPB with the valence band edge of $CH_3NH_3PbI_3$ (Kim et al., 2015). However, there is no report about the NPB/MoO_3 double-layer with NPB contact with photoactive layer in polymer solar cells. In this work, efficient polymer solar cells were fabricated with P3HT: PCBM as photoactive layer and the insertion of NPB layer between active layer and MoO_3 layer as double-layer HTL. The effect of NPB thickness on the performance of device was investigated. The technique of transient photocurrent and electrochemical impedance has been carried out to study the role of this double-layer buffer on the performance of polymer solar cells.

2. Experimental section

Materials. P3HT with regioregularity better than 98% was purchased from Rieke metals, PCBM was purchased from American Dye Source. 1,2-dichloro-benzene (DCB, anhydrous, 99%), NPB, MoO_3, polyethylenimine, 80% ethoxylated (PEIE) (Mw = 70,000 g/mol), dissolved in H_2O with a concentration of 35–40 wt% were bought from Sigma Aldrich.

Device fabrication. Fig. 1(a) depicts the structure of the planar heterojunction device with ITO/PEIE/P3HT:$PC_{61}BM$/NPB(X)/MoO_3/Ag, in which X are 0, 1, 3, 5, 8 nm, respectively. The schematic diagram of the relative energy levels of each layer is shown in Fig. 1(b). A prepatterned ITO glass substrate with a sheet resistance about 15 Ω/square was ultrasonically cleaned for 20 min by sequentially ultrasonic cleaning in detergent, acetone, and deionized water, respectively. After oxygen plasma treatment, the ITO was covered by spin coating a 5 nm thick PEIE layer on top of it (Li et al., 2014b). Then, the active layer on the PEIE was prepared by spin-coating a P3HT:PCBM (1:1 w/w) DCB solution with a concentration of 34 mg/ml without any additives at speed of 870 rpm for 60 s. Next, the samples were then transferred into a vacuum chamber and covered by 0, 1, 3, 5, or 8 nm NPB on P3HT:PCBM active layer by thermal evaporation. Finally, 7 nm thick MoO_3 and 100 nm thick Ag electrodes were thermally evaporated at rates of 0.02 and 0.1 nm/s, respectively, through a shadow mask at a pressure of $\sim 10^{-7}$ mbar. These full devices were marked as 0-NPB, 1-NPB, 3-NPB, 5-NPB, 8-NPB, respectively. The cell area, as defined by the overlap between ITO and Ag electrodes, is 0.09 cm^2. The deposition rate was monitored in-situ by a calibrated quartz oscillator. A device with only NPB as HTL was prepared to compare with other devices (marked as pure-NPB).

Device characterization. The current-voltage (I-V) measurements were carried out by Keithley 2400 under 100 $mW \cdot cm^{-2}$ (AM 1.5 G) simulated sunlight from a Newport solar simulator (94043A). The external quantum efficiencies (EQE) of the devices were calculated from the photocurrent measured by a lock-in amplifier (SR-830). The light intensity was measured using a calibrated Si detector. Transient photocurrent (TPC) was obtained by an Agilent oscilloscope with a bandwidth of 1 GHz with pulsed laser from the ITO side. The wavelength of the pulse laser is 532 nm and the silver electrode was grounded. The electrochemical impedance spectra (EIS) was measured using an electrochemical workstation (Shanghai Chen Hua, CHI 660D) with the standard AM15.G 100 $mW \cdot cm^{-2}$ illumination.

3. Results and discussion

The I-V characteristics of inverted P3HT:PCBM solar cells with different HTL were measured under 100 $mW \cdot cm^{-2}$ AM 1.5G solar illumination. All the devices showed reasonable performance, as shown in Fig. 2(a) and were summarized in Table 1. Data in parentheses are the best performance of inverted solar cells. R_s and R_{sh} are extracted from the I-V characteristics of these devices shown in Fig. 1(a) using the analytical five point method (Cotfas et al., 2013). With only MoO_3 HTL (0-NPB), the device gives a PCE of 3.20 ± 0.27%, with the short circuit current (J_{sc}) of 8.54 ± 0.36 $mA \cdot cm^{-2}$, the open-circuit voltage (V_{oc}) of 0.59 ± 0.01 V, and the fill factor (FF) of 63 ± 2%. While the device with only NPB HTL yields a PCE of 1.84 ± 0.43%, with J_{sc} of 7.64 ± 0.61 $mA \cdot cm^{-2}$, V_{oc} of 0.52 ± 0.02 V, and FF of 48 ± 3%. By inserting NPB HTL between MoO_3 and the photoactive layer, the performance of the inverted cells is remarkably enhanced. The J_{sc} increases from 8.54 ± 0.36 to 10.04 ± 0.39 $mA \cdot cm^{-2}$ as the thickness of NPB

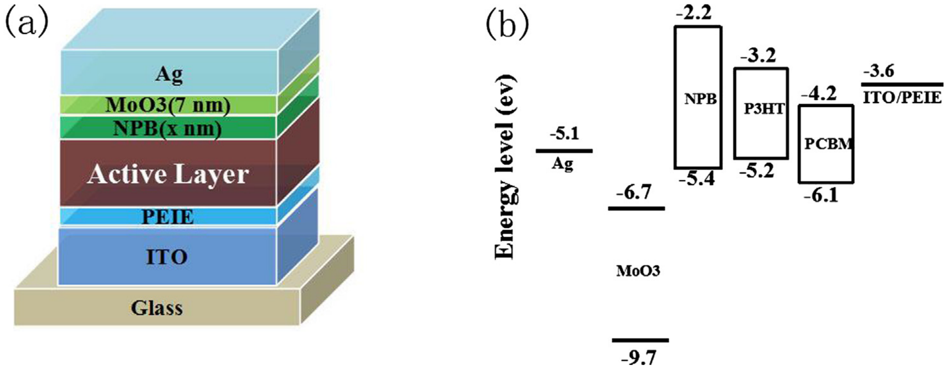

Fig. 1. (a) Device structure of the fabricated polymer solar cell. (b) The schematic diagram of the relative energy level for each layer.

Download English Version:

https://daneshyari.com/en/article/7935037

Download Persian Version:

https://daneshyari.com/article/7935037

Daneshyari.com